



Contents lists available at ScienceDirect

## Metabolism Clinical and Experimental

journal homepage: [www.metabolismjournal.com](http://www.metabolismjournal.com)

## UCP1-dependent and UCP1-independent metabolic changes induced by acute cold exposure in brown adipose tissue of mice

Yuko Okamatsu-Ogura<sup>a,\*</sup>, Masashi Kuroda<sup>b</sup>, Rie Tsutsumi<sup>b</sup>, Ayumi Tsubota<sup>a</sup>, Masayuki Saito<sup>a</sup>, Kazuhiro Kimura<sup>a</sup>, Hiroshi Sakaue<sup>b</sup><sup>a</sup> Laboratory of Biochemistry, Faculty of Veterinary Medicine, Hokkaido University, Sapporo 060-0818, Japan<sup>b</sup> Department of Nutrition and Metabolism, Institute of Health Biosciences, Tokushima University Graduate School, Tokushima 770-8503, Japan

## ARTICLE INFO

## Article history:

Received 27 July 2020

Accepted 28 September 2020

## Keywords:

Brown adipose tissue  
Uncoupling protein 1  
Cold exposure  
Metabolomics  
GeneChip array

## ABSTRACT

**Background:** Brown adipose tissue (BAT) is a site of metabolic thermogenesis mediated by mitochondrial uncoupling protein 1 (UCP1) and represents a target for a therapeutic intervention in obesity. Cold exposure activates UCP1-mediated thermogenesis in BAT and causes drastic changes in glucose, lipid, and amino acid metabolism; however, the relationship between these metabolic changes and UCP1-mediated thermogenesis is not fully understood.

**Methods:** We conducted metabolomic and GeneChip array analyses of BAT after 4-h exposure to cold temperature (10 °C) in wild-type (WT) and UCP1-KO mice.

**Results:** Cold exposure largely increased metabolites of the glycolysis pathway and lactic acid levels in WT, but not in UCP1-KO, mice, indicating that aerobic glycolysis is enhanced as a consequence of UCP1-mediated thermogenesis. GeneChip array analysis of BAT revealed that there were 2865 genes upregulated by cold exposure in WT mice, and 838 of these were upregulated and 74 were downregulated in UCP1-KO mice. Pathway analysis revealed the enrichment of genes involved in fatty acid (FA)  $\beta$  oxidation and triglyceride (TG) synthesis in both WT and UCP1-KO mice, suggesting that these metabolic pathways were enhanced by cold exposure independently of UCP1-mediated thermogenesis. FA and cholesterol biosynthesis pathways were enhanced only in UCP1-KO mice. Cold exposure also significantly increased the BAT content of proline, tryptophan, and phenylalanine amino acids in both WT and UCP1-KO mice. In WT mice, cold exposure significantly increased glutamine content and enhanced the expression of genes related to glutamine metabolism. Surprisingly, aspartate was almost completely depleted after cold exposure in UCP1-KO mice. Gene expression analysis suggested that aspartate was actively utilized after cold exposure both in WT and UCP1-KO mice, but it was replenished from intracellular *N*-acetyl-aspartate in WT mice.

**Conclusions:** These results revealed that cold exposure induces UCP1-mediated thermogenesis-dependent glucose utilization and UCP1-independent active lipid metabolism in BAT. In addition, cold exposure largely affects amino acid metabolism in BAT, especially UCP1-dependently enhances glutamine utilization. These results contribute a comprehensive understanding of UCP1-mediated thermogenesis-dependent and thermogenesis-independent metabolism in BAT.

© 2020 The Author(s). Published by Elsevier Inc. This is an open access article under the CC BY-NC-ND license (<http://creativecommons.org/licenses/by-nc-nd/4.0/>).

**Abbreviations:** ANOVA, Analysis of variance; AST, aspartate aminotransferase; ASPA, aspartoacylase; BAT, brown adipose tissue;  $\beta$ -AR,  $\beta$ -adrenergic receptor; BCAA, branched-chain amino acids; F-6-P, fructose 6-phosphate; FA, Fatty acid; FBP, fructose 1,6-bisphosphate; G-1-P, Glucose 1-phosphate; G-6-P, glucose 6-phosphate; GSH, glutathione; GSSG, glutathione disulfide; GWAT, perigonadal white adipose tissue; IWAT, inguinal white adipose tissue; MDH, malate dehydrogenase; ME, malic enzyme; Asp-NAT, *N*-acetyl-aspartate synthetase; PET-CT, positron emission tomography-computed tomography; SNS, sympathetic nervous system; TCA, tricarboxylic acid; TG, triglyceride; UCP1, uncoupling protein 1; WAT, white adipose tissue; WT, wild-type.

\* Corresponding author.

E-mail address: [y-okamatsu@vetmed.hokudai.ac.jp](mailto:y-okamatsu@vetmed.hokudai.ac.jp) (Y. Okamatsu-Ogura).

## 1. Introduction

Obesity is a major risk factor for metabolic disorders, such as type 2 diabetes, hyperlipidemia, and nonalcoholic fatty liver disease. Brown adipose tissue (BAT) has attracted attention as a target for therapeutic intervention in obesity [1,2]. BAT is a tissue specialized for metabolic thermogenesis mediated through mitochondrial uncoupling protein 1 (UCP1), which uncouples respiration from ATP synthesis [3]. UCP1 activity is controlled by the sympathetic nervous system (SNS); physiological stimuli such as cold exposure and several kinds of stress [4,5] activate sympathetic nerves that innervate BAT, which induces the activation of  $\beta$ -adrenergic receptor ( $\beta$ -AR) and downstream signaling

pathway, ultimately activating UCP1 activity. UCP1-mediated thermogenesis is important in maintaining body temperature in cold environments [6] and during the postnatal period [7], as well as in regulating adiposity. The activation of UCP1-mediated thermogenesis increases whole body energy expenditure and leads to a reduction of body fat in both rodents and humans [8–11].

SNS stimulation induces drastic metabolic changes in BAT, simultaneous with the activation of UCP1-mediated thermogenesis. When  $\beta$ -AR is activated by norepinephrine, the intracellular cAMP-protein kinase A pathway is activated, which leads to the phosphorylation of adipose triglyceride lipase and hormone-sensitive lipase, resulting in the lipolysis of intracellular lipid droplets. Fatty acids (FAs) directly activate the UCP1 function [12,13], and at the same time serve as substrates for thermogenesis. SNS activation also causes lipolysis in white adipose tissue (WAT) through a similar intracellular signaling pathway, and the liberated FAs are mobilized into circulation as free FAs, which can be incorporated into BAT and used for thermogenesis. BAT also incorporates FAs liberated from the circulating triglyceride-rich lipoproteins through the action of lipoprotein lipase [14,15]. Lipolysis is essential for BAT thermogenesis in rodents [16] and humans [17], although whether the intracellular lipolysis in brown adipocytes is indispensable or can be substituted by the incorporation of FAs from circulation is controversial [18,19].

In addition to lipid metabolism, BAT substantially increases glucose utilization upon SNS activation. In rodents, this glucose uptake is ameliorated by denervation of sympathetic nerves [20] or genetic deletion of *Ucp1* [21], indicating that this pathway is fully dependent on UCP1-mediated thermogenesis. Glucose uptake is also reported to be AMPK-dependent mechanism [21,22], suggesting that glucose is used to replenish ATP through aerobic glycolysis to compensate for the decreased ATP production in mitochondria caused by UCP1 uncoupling. Indeed, *in vitro* [23] and *in vivo* [24] experiments have shown that inhibition of glycolysis impairs BAT thermogenesis. Thus, it has been accepted that cold-induced glucose uptake in BAT is dependent on UCP1 activity.

Although the studies on amino acid metabolism in BAT are limited, it has been reported that cold exposure greatly alters the makeup of amino acid pools and the activity of enzymes involved in amino acid metabolism in BAT [25–27]. Lopez-Soriano et al. evaluated the net uptake and release of amino acids in BAT by measuring arteriovenous amino acid concentration difference and found that 4-h cold exposure in rats increased BAT influx of amino acids, such as glutamine and branched-chain amino acids (BCAAs), accounting for about one-third of the energy supplied by glucose to the tissue [25]. The authors suggested that the efflux of glycine and proline partially compensated for the positive nitrogen balance induced by cold exposure in BAT. Consistent with their findings, it was recently reported that BCAAs are actively utilized in BAT mitochondria for thermogenesis upon cold exposure in mice [28]. Thus, amino acids, as well as glucose and FAs, are likely to be important energy substrates in BAT during cold exposure; however, the relationship of amino acid metabolism to UCP1-mediated thermogenesis is still unclear.

The thermogenic function of BAT is supported by the metabolic characteristics of this tissue both in rodents and humans and these characteristics were utilized to evaluate the volume and activity of human BAT. For example, positron emission tomography-computed tomography (PET-CT) imaging using the glucose analog 18F-fluorodeoxyglucose as a tracer is used to assess BAT activity [9,29–31]. However, some studies suggest that this method does not always reflect BAT activity [30,31]. It is also reported that the lipolysis-driven high concentration of FAs promotes insulin secretion, which may contribute to the increase in the uptake of not only glucose but also FAs and amino acids in BAT through a UCP1-independent mechanism [32]. Other tracers, such as a long-chain FA analog 18F-fluoro-6-thia-heptadecanoic acid, have been used to estimate FA uptake by BAT [33]; however, whether FA utilization in BAT is dependent on UCP1-mediated thermogenesis and reflects

the BAT activity is still unclear. Therefore, understanding whether cold-induced metabolic changes reflect BAT thermogenesis or occur independently of the thermogenic function of BAT is important. In this study, we conducted a comprehensive analysis of cold-induced changes in metabolite composition and gene expression in BAT using wild-type (WT) and UCP1-KO mice.

## 2. Materials and methods

### 2.1. Animals

The experimental procedures and care of animals were approved by the Animal Care and Use Committee of Hokkaido University. All experiments using mice were conducted in an animal facility approved by the Association for Assessment and Accreditation of Laboratory Animal Care International. Mice were bred and housed in plastic cages placed in a temperature-controlled room at  $23 \pm 2 \text{ }^\circ\text{C}$  with a 12:12 h light/dark cycle and given free access to laboratory chow (Oriental Yeast, Tokyo, Japan) and tap water.

For the first experiment, male C57BL/6J mice (5 weeks old) were purchased from Japan SLC Inc. (Hamamatsu, Japan). After the 1-week acclimation period, mice were singly housed and randomly divided into three experimental groups. Control mice were kept at room temperature,  $23 \pm 2 \text{ }^\circ\text{C}$ . The other two groups of mice were exposed to cold temperature ( $4 \text{ }^\circ\text{C}$ ) for 4 or 24 h. For the second experiment, UCP1-KO (*Ucp1*<sup>-/-</sup>) mice were kindly provided by Dr. L. Kozak (Pennington Biomedical Research Center, Baton Rouge, LA, USA). UCP1-KO mice and their WT littermates (10 weeks old) were singly housed, and control mice were kept at room temperature ( $23 \pm 2 \text{ }^\circ\text{C}$ ), whereas the other mice were exposed to cold temperature ( $10 \text{ }^\circ\text{C}$ ) for 4 h. Mice were given free access to laboratory chow during cold exposure. Mice were euthanized via cervical dislocation, and interscapular BAT and inguinal and perigonadal WAT were dissected and transferred into liquid nitrogen or RNAlater (Thermo Fisher Scientific, Gaithersburg, MD, USA). Five mice for each group were used. Sampling was conducted between 1:00 p.m. and 3:00 p.m.

### 2.2. Metabolomic analyses

Targeted profiling of amino acid metabolites was performed by capillary electrophoresis time-of-flight mass spectrometry (CE  $\pm$  TOF/MS) using an Agilent 7100 CE Capillary Electrophoresis system equipped with an Agilent 6230 time-of-flight mass spectrometer (Agilent Technologies, Palo Alto, CA, USA) according to the methods described previously [34]. In brief, frozen adipose tissue samples were homogenized in methanol containing internal standards (H3304-1002, Human Metabolome Technology Inc., Yamagata, Japan); subsequently, both chloroform and Milli-Q water were added to the sample solution. The solution was centrifuged, and the aqueous fraction was centrifugally filtered through an Ultrafree MC-PLHCC filter (Human Metabolome Technology Inc.). The filtrate was dried and dissolved in Milli-Q water containing reference compounds (H3304-1004, Human Metabolome Technology Inc.). CE-TOF/MS conditions were as reported previously [35]. Cationic metabolites were analyzed using a fused silica capillary (50- $\mu\text{m}$  interior diameter (i.d.),  $\text{\AA}$ -, 80-cm total length) with cation buffer solution (Human Metabolome Technologies) as the electrolyte. The sample was injected at a pressure of 50 mbar for 10 s. The applied voltage was set at 27 kV. Electrospray ionization (ESI)-mass spectrometry was conducted in the positive ion mode, and the capillary voltage was set at 4000 V. To detect anionic metabolites, a cationic polymer capillary (50- $\mu\text{m}$  i.d.  $\text{\AA}$ -, 80-cm total length) was used with anionic buffer (H3302-1021). The sample was injected at a pressure of 50 mbar for 25 s, and the applied voltage was 30 kV. ESI-TOF/MS was set in the negative ion mode with 3.5 kV for anionic metabolites.

The spectrometer was scanned from 50 to 1000 *m/z*. An automatic recalibration of each acquired spectrum was performed using the

masses of reference standards. For CE-MS system control and data acquisition, we used an Agilent MassHunter software for TOF/MS (Agilent Technologies). All target metabolites were identified by matching their *m/z* values and migration times with the normalized *m/z* values and migration times of corresponding authentic standard compounds.

## 2.3. Affymetrix GeneChip array analysis

### 2.3.1. Labeling protocol

Total RNA was extracted using TRIzol reagent (Thermo Fisher Scientific) according to the manufacturer's instructions. Cyanine-3 (Cy3)-labeled cRNA was prepared from 150 ng RNA using the One-Color Low Input Quick Amp Labeling kit (Agilent) according to the manufacturer's instructions, followed by RNAeasy column purification (QIAGEN, Hilden, Germany). Dye incorporation and cRNA yield were verified with the NanoDrop ND-1000 Spectrophotometer.

### 2.3.2. Hybridization protocol

Cy3-labeled cRNA (600 ng; specific activity >6 pmol Cy3/μg cRNA) was fragmented at 60 °C for 30 min in a reaction volume of 25 μl, containing 25 X Agilent fragmentation buffer and 10 X Agilent blocking agent, following the manufacturer's instructions. On the completion of the fragmentation reaction, 25 μl of 2× Agilent hybridization buffer was added to the fragmentation mixture and hybridized to Agilent SurePrint GE Unrestricted Microarrays (G2519F) for 17 h at 65 °C in a rotating Agilent hybridization oven. After hybridization, microarrays were washed for 1 min at room temperature with GE Wash Buffer 1 (Agilent) and 1 min with 37 °C GE Wash Buffer 2 (Agilent) and then dried immediately.

### 2.3.3. Scan protocol

Slides were scanned immediately after washing on the Agilent DNA Microarray Scanner (G2505C) using the one-color scan setting for 8x60K array slides (scan area, 61 × 21.6 mm; scan resolution, 3 μm; dye channel, green; green PMT, 100%).

### 2.3.4. Data processing

The scanned images were analyzed with Feature Extraction Software 10.7.1.1 (Agilent) using default parameters (protocol GE1\_107\_Sep09 and Grid: 028282\_D\_F\_20110531) to obtain background subtracted and spatially detrended processed signal intensities. Features flagged in Feature Extraction as Feature Non-uniform outliers were excluded. Data were analyzed using GeneSpring software (Agilent).

## 2.4. Real-time PCR

Total RNA was extracted using TRIzol reagent (Thermo Fisher Scientific) according to the manufacturer's instructions, and reverse-transcribed using a 15-mer oligo(dT) adaptor primer and M-MLV reverse transcriptase (Promega, Madison, WI, USA). Real-time PCR was performed on a fluorescence thermal cycler (LightCycler system; Roche, Mannheim, Germany) using Brilliant III Ultra-Fast SYBR Green QPCR Mater Mixes (Agilent Technologies). The relative expression levels were calculated by the comparative cycle threshold ( $\Delta\Delta C_t$ ) method using *TFIIB* as the housekeeping gene. The primers used are listed in Table 1.

## 2.5. Data analysis

Values are expressed as mean ± SE. Statistical analyses were performed using one-way or two-way analysis of variance (ANOVA), followed by the Tukey's Honest Significant Difference (HSD) post-hoc test.

**Table 1**  
Primer sequences for quantitative real-time PCR.

Gene symbol: forward, and reverse primer sequence
Acaca: 5'-TCGGCACATGGAGATGTACG-3', 5'-GATCTACCCGACGATGGTT-3'
Acly: 5'-TCAGTCCCAAGTCCAAGATCC-3', 5'-TCTCGGGAACACACGTAGTC-3'
Aspa: 5'-TGGAGACATGGCTGCTGTTATT-3', 5'-ATCTCCAGGTCGAATGGTTT-3'
Fasn: 5'-AAGTACCATGGCAACGTGAC-3', 5'-CAATGATGTGCACAGACACC-3'
Gclc: 5'-AAGGACGTGCTCAAGTGGG-3', 5'-AGGCGTTCCTCGATCATGT-3'
Gls2: 5'-GGTTCAGCAATGCCACATTC-3', 5'-TCACAGGTAACCTCCACAGA-3'
Glud1: 5'-ACTGACGTGAGTGTGGATGA-3', 5'-TCCATAGTGAACCTCCGTGT-3'
Gss: 5'-GCATGGGTCGTACCGAAG-3', 5'-TATGGCTGCTTTGCCAGTT-3'
Me1: 5'-GACCCGATCTCAACAAGGAC-3', 5'-TCATTTCTGCTTCAGGTTCCA-3'
Scd1: 5'-CCAAGCTGGAGTACGTCTGG-3', 5'-CAGAGCGTGGTCATGTAGT-3'
TFIIB: 5'-TGGAGATTGTCCACCATGA-3', 5'-GAATGCCAAACTCATCAAAC-3'

## 3. Results

First, we examined the effect of cold exposure (4 °C) for 4 and 24 h on the carbohydrate metabolite contents in BAT and WAT of inguinal (IWAT) and perigonadal (GWAT) depots (Fig. 1A, Table 2). In BAT, 4-h cold exposure tended to increase metabolites in the glycolysis pathway, including glucose 6-phosphate (G-6-P), fructose 6-phosphate (F-6-P), fructose 1,6-bisphosphate (FBP), and phosphoenolpyruvic acid, and significantly increased lactic acid. These changes were sustained after 24-h cold exposure, indicating the continuous enhancement of aerobic glycolysis. Metabolites of the pentose phosphate pathway, including 6-phosphogluconic acid, ribulose 5-phosphate, and sedoheptulose 7-phosphate, were gradually increased by cold exposure, being significantly higher after 24-h exposure compared to the control group. After 4 h, intermediates of the tricarboxylic acid (TCA) cycle, except for only isocitric acid, also showed an increase, which sustained at 24-h cold exposure. Glucose 1-phosphate (G-1-P) increased transiently at 4 h but decreased at 24 h. Glycerol 3-phosphate increased after cold exposure, being significantly higher at 24-h exposure compared to the control.

In WAT of the control group, most of the carbohydrate metabolites were significantly lower than that in BAT. In IWAT, 4-h cold exposure did not cause significant changes in carbohydrate metabolite contents, but 24-h exposure led to a significant increase in metabolites of glycolysis and the pentose phosphate pathway, demonstrating comparable levels to those in BAT. Cold exposure for 24 h showed a significant increase in some of the TCA cycle intermediates compared to the control group, but the levels of these intermediates were still very low compared to those in BAT. Cold exposure caused slight changes in metabolite contents in GWAT; however, the responses were much weaker than those in IWAT.

The effect of cold exposure on amino acid content was also examined (Fig. 1B, Table 3). In BAT, 4-h cold exposure largely increased the levels of most of the amino acids examined, and this change was sustained after 24 h. Only the levels of glycine were kept constant during cold exposure. In IWAT of the control group, the basal levels of amino acids, except for methionine and lysine, were significantly lower than those in control BAT. Cold exposure for 4 h significantly increased the levels of alanine, threonine, and isoleucine, but failed to induce changes in other amino acids, whereas 24-h exposure significantly increased levels of most of the amino acids. The levels of glycine, glutamine, glutamate, and methionine were not changed during cold exposure. Basal levels of amino acids in GWAT except for methionine were significantly lower than those in BAT, and approximately half of the amino acids showed a significant increase at 24 h of cold exposure. These results indicate that cold exposure induces drastic changes in amino acid levels in adipose tissues. In addition, amino acid levels were already altered 4 h after the start of cold exposure in BAT, but the response in WAT required a longer period of exposure.

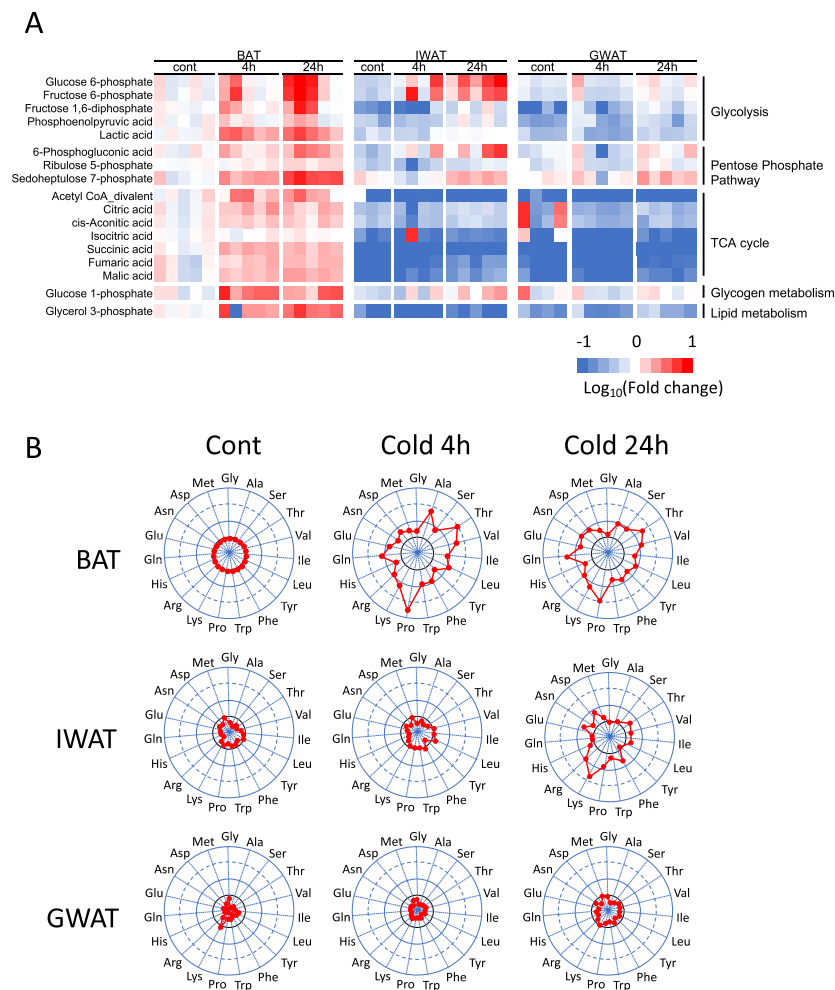


**Fig. 1.** Effect of cold exposure on metabolites in adipose tissue of wild-type mice. Male C57BL/6J mice (6 weeks old) were exposed to cold (4 °C) for 4 or 24 h. Control mice were kept at room temperature (23 °C). Interscapular brown adipose tissue (BAT) and inguinal and perigonadal white adipose tissue (IWAT and GWAT, respectively) were collected, and the concentration of each metabolites was measured. (A) Carbohydrate metabolite levels in BAT, IWAT, and GWAT are expressed in a heat map as the log value of fold change compared to the values in BAT of control mice. (B) Amino acid contents in tissues are expressed as fold change compared to the contents in BAT of control mice. Small circles and solid lines indicate one- and twofold levels, respectively, while dotted lines indicate threefold levels. Values represent means of 3–5 samples in each group.

As the content of carbohydrate metabolites and amino acids in BAT changed drastically after 4-h cold exposure, we next evaluated if these metabolic changes were dependent on UCP1 activity using UCP1-KO mice. Since UCP1-KO mice are cold-intolerant [6], a milder cold condition (10 °C) was chosen for this experiment. In WT mice, mild cold exposure induced a tendency of increase in metabolites of the glycolytic pathway and a significant increase in lactic acid, similar to the 4 °C condition in WT mice (Fig. 1A), although the degree of induction was slightly reduced (Fig. 2A). In contrast, glycolysis metabolites including G-6-P, F-6-P, and FBP significantly decreased in UCP1-KO mice. Lactic acid levels did not change after cold exposure, although the basal level tended to be higher in UCP1-KO mice compared to that in WT mice (Fig. 2B). Metabolites of the pentose phosphate pathway tended to increase in WT mice, but changes were negligible in UCP1-KO mice after cold exposure. Intermediates of the TCA cycle upstream of  $\alpha$ -ketoglutaric acid (citric acid, cis-aconitic acid, and isocitric acid) were tended to increase in both WT and UCP1-KO mice; however, intermediates downstream of  $\alpha$ -ketoglutaric acid (succinic acid, fumaric acid, and malic acid) showed significant increase only in WT, but not in UCP1-KO, mice after cold exposure. G-1-P increased after cold exposure in WT, but not in UCP1-KO, mice. Glycerol 3-phosphate was significantly increased in WT mice and decreased in UCP1-KO mice after cold exposure.

The effect of mild cold exposure (10 °C) on amino acids in WT mice was minimal but demonstrated a similar pattern to that observed at 4 °C (Figs. 1B, 3A). The basal level of amino acids was similar between WT and UCP1-KO mice. Proline, tryptophan, and phenylalanine levels were significantly increased in both WT and UCP1-KO mice after cold exposure. Cold exposure significantly increased glutamine specifically in WT mice and significantly increased BCAAs, including valine, leucine, and isoleucine, specifically in UCP1-KO mice. Surprisingly, aspartate was almost completely depleted after cold exposure in UCP1-KO mice.

GeneChip array analysis of BAT revealed that there were 2865 genes upregulated by cold exposure in WT mice, and 838 of these genes were also upregulated and 74 were downregulated in UCP1-KO mice (Fig. 4A). Pathway analysis of gene sets upregulated by cold exposure revealed the enrichment of genes involved in glycolysis and glycogen metabolism in WT mice (Fig. 4B), consistent with the observed metabolite changes. In UCP1-KO mice, although the levels of metabolites of the glycolysis pathway were significantly decreased and metabolites of the pentose phosphate pathway were not changed, the gene expression of enzymes in these pathways seemed to be enhanced by cold exposure. Activation of the “oxidative stress” and “selenium metabolism selenoproteins” pathways in WT mice suggests the enhanced glutathione disulfide (GSSG) synthesis from glutathione (GSH), which requires selenium. In WT

**Table 2**  
Carbohydrate metabolites in adipose tissues.

Metabolite (n mole/g tissue)	BAT			IWAT			GWAT			2-way ANOVA p-value		
	Cont	4h	24h	Cont	4h	24h	Cont	4h	24h	BAT vs	IWAT vs	GWAT vs
										IWAT	GWAT	
<b>Glycolysis</b>												
Glucose 6-phosphate	14 ± 2.4	26 ± 8.5	100 ± 42	7.1 ± 0.3	33 ± 18	70 ± 21	11 ± 0.7	14 ± 4.4	16 ± 2.1			
Fructose 6-phosphate	3.5 ± 0.5	8.0 ± 3.5	21 ± 8.7	1.7 ± 0.2	11 ± 6	11 ± 3	2.2 ± 0.2	2.6 ± 0.8	3.3 ± 0.4			
Fructose 1,6-diphosphate	31 ± 2.3	55 ± 12	109 ± 44	5.2 ± 0.7	6 ± 4	25 ± 6	3.3 ± 2.2	11 ± 3.9	22 ± 2.8	<0.01	<0.01	<0.01
Dihydroxyacetone phosphate	54 ± 11	79 ± 6.3	122 ± 29	2.0 ± 0.5	1 ± 0	4 ± 0	0.6 ± 0.2	0.9 ± 0.2	1.2 ± 0.2	<0.01	<0.01	<0.01
Glyceraldehyde 3-phosphate	1.2 ± 0.3	1.6 ± 0.4	1.0 ± 0.4	2.6 ± 1.3	0 ± 0	1 ± 0	0.6 ± 0.1	0.3 ± 0.1	1.2 ± 0.8			
3-Phosphoglyceric acid	60 ± 8.7	76 ± 7.5	82 ± 14	12 ± 3.2	9 ± 4	7 ± 5	10 ± 3.7	14 ± 5.2	10 ± 6.6	<0.01	<0.01	<0.01
2-Phosphoglyceric acid	6.1 ± 0.7	7.9 ± 0.8	9.5 ± 1.9	1.5 ± 0.4	2 ± 0	1 ± 0	1.5 ± 0.1	1.3 ± 0.4	0.8 ± 0.5	<0.01	<0.01	<0.01
Phosphoenolpyruvic acid	3.4 ± 0.4	4.1 ± 0.6	5.1 ± 1.1	1.4 ± 0.3	1 ± 0	3 ± 1	0.8 ± 0.1	1.5 ± 0.4	1.7 ± 0.3	<0.01	<0.01	<0.01
Lactic acid	6,313 ± 623	19,381 ± 22,273	3,521 ± 625	3,521 ± 625	3,703 ± 780	6,187 ± 184	2,423 ± 383	2,044 ± 508	3,043 ± 210	<0.01	<0.01	<0.01
<b>Pentose phosphate pathway</b>												
6-Phosphogluconic acid	2.7 ± 0.3	4.2 ± 0.6	7.0 ± 1.2	1.1 ± 0.2	4 ± 1	8 ± 3	1.9 ± 0.3	1.7 ± 0.7	3.5 ± 0.5			
Ribulose 5-phosphate	54 ± 2.1	61 ± 4.3	76 ± 3.4	26 ± 2.7	17 ± 6	36 ± 3	41 ± 5.8	38 ± 10	54 ± 7.3	<0.01	<0.01	<0.01
Sedoheptulose 7-phosphate	5.2 ± 1.1	13 ± 1.0	29 ± 2.8	6.2 ± 0.9	4 ± 1	11 ± 1	5.9 ± 0.4	5.8 ± 1.3	10 ± 1.3	*+	<0.01	<0.01
<b>TCA cycle</b>												
Acetyl CoA, divalent	1.7 ± 0.3	4.1 ± 1.0	4.2 ± 0.9	0.05 ± 0.03	0.09 ± 0.03	0.06 ± 0.02s	0.1 ± 0.1	0.1 ± 0.0	0.1 ± 0.0	<0.01	<0.01	<0.01
Citric acid	222 ± 33	442 ± 53	394 ± 41	82 ± 6.3	64 ± 18	122 ± 6.6	599 ± 344	56 ± 3.4	84 ± 10	0.044	0.035	
cis-Aconitic acid	2.3 ± 0.3	3.6 ± 0.2	3.6 ± 0.3	1.0 ± 0.1	0.7 ± 0.1	1.2 ± 0.1	6.0 ± 3.5	0.7 ± 0.1	0.8 ± 0.1			
Isocitric acid	14 ± 1.1	11 ± 3.1	15.4 ± 0.7	2.1 ± 0.5	24 ± 23	2.1 ± 0.1	10 ± 5.3	1.0 ± 0.0	1.6 ± 0.2			
Succinic acid	1,052 ± 105	2,200 ± 115	1,955 ± 113	53 ± 6.1	46 ± 4	55 ± 5.9	48 ± 8.5	39 ± 4.9	44 ± 12	<0.01	<0.01	<0.01
Fumaric acid	188 ± 43	316 ± 29	351 ± 18	14 ± 0.5	17 ± 2	34 ± 3.8	16 ± 3.1	13 ± 1.4	19 ± 1.8	<0.01	<0.01	<0.01
Malic acid	515 ± 114	926 ± 41	1,123 ± 61	36 ± 1.6	64 ± 9	115 ± 14	53 ± 19	48 ± 5.7	73 ± 6.4	<0.01	<0.01	<0.01
<b>Glycogen metabolism</b>												
Glucose 1-phosphate	3.6 ± 0.6	16 ± 3.1	11 ± 2.5	2.0 ± 0.2	3.4 ± 1.2	6.0 ± 1.1	5.6 ± 2.9	2.9 ± 0.8	3.9 ± 0.5	<0.01	<0.01	<0.01
<b>Glycerol metabolism</b>												
Glycerol 3-phosphate	472 ± 37	1,237 ± 435	1,964 ± 254	56 ± 26	16 ± 4	50 ± 14	104 ± 25	114 ± 41	163 ± 34	<0.01	<0.01	<0.01

\* p<0.05 vs cont

+ p<0.05 vs 4h

**Table 3**  
Amino acids in adipose tissues.

Amino acid (n mole/g tissue)	BAT			IWAT			GWAT			2-way ANOVA p-value		
	Cont	4h	24h	Cont	4h	24h	Cont	4h	24h	BAT vs IWAT	BAT vs GWAT	IWAT vs GWAT
Gly	507 ± 28	673 ± 61	588 ± 57	328 ± 29	296 ± 30	417 ± 40	414 ± 40	325 ± 45	442 ± 38	<0.01	<0.01	
Ala	750 ± 181	1,993 ± 83 *	1,420 ± 125 *†	330 ± 39	592 ± 51 *	929 ± 77 *†	207 ± 13	288 ± 23 *	392 ± 16 *†	<0.01	<0.01	
Ser	205 ± 17	359 ± 22 *	383 ± 30 *	129 ± 12	129 ± 10	206 ± 11	83 ± 9	82 ± 9	129 ± 10 *†	<0.01	<0.01	<0.01
Pro	84 ± 9	286 ± 19 *	240 ± 18 *	52 ± 5	74 ± 7	145 ± 13	36 ± 7	41 ± 6	63 ± 5 *	<0.01	<0.01	0.04
Val	102 ± 8	250 ± 5 *	213 ± 14 *	69 ± 7	108 ± 8	186 ± 17	39 ± 3	57 ± 9	80 ± 5 *	<0.01	<0.01	<0.01
Thr	174 ± 12	504 ± 33 *	432 ± 36 *	87 ± 8	135 ± 14 *	226 ± 9	54 ± 3	83 ± 12	135 ± 13 *†	<0.01	<0.01	
Ile	36 ± 2	66 ± 3	59 ± 3	30 ± 2	37 ± 4	60 ± 5	21 ± 3	18 ± 3	26 ± 2 *†	<0.01	<0.01	
Leu	73 ± 5	153 ± 6 *	133 ± 10 *	64 ± 4	88 ± 8	122 ± 9	34 ± 5	39 ± 7	56 ± 4 *	<0.01	<0.01	<0.01
Asn	40 ± 3	54 ± 4	75 ± 5	30 ± 3	30 ± 3	54 ± 3	16 ± 2	16 ± 2	33 ± 2 *†	<0.01	<0.01	<0.01
Asp	253 ± 9	407 ± 30 *	456 ± 38 *	177 ± 18	149 ± 20	253 ± 17	67 ± 4	84 ± 11	144 ± 14 *†	<0.01	<0.01	<0.01
Gln	869 ± 97	1,825 ± 74 *	2,128 ± 264 *	484 ± 47	413 ± 37	600 ± 99	218 ± 100	323 ± 61	570 ± 82 *	<0.01	<0.01	
Lys	132 ± 10	290 ± 56 *	300 ± 14 *	106 ± 10	115 ± 10	329 ± 83	144 ± 56	77 ± 21	129 ± 11		<0.01	
Glu	789 ± 97	1,333 ± 92 *	1,332 ± 82 *	456 ± 37	480 ± 39	560 ± 149	175 ± 39	297 ± 30	425 ± 28 *†	<0.01	<0.01	0.02
Met	28 ± 2	40 ± 3	40 ± 3	28 ± 2	27 ± 4	45 ± 9	14 ± 2	17 ± 3	26 ± 2			
His	40 ± 3	55 ± 3	60 ± 5	17 ± 7	22 ± 2	38 ± 4	3 ± 3	14 ± 3	24 ± 4 *	<0.01	<0.01	
Phe	38 ± 2	71 ± 3	66 ± 4	28 ± 4	40 ± 2	67 ± 4	14 ± 3	21 ± 3	31 ± 2 *†	<0.01	<0.01	<0.01
Arg	57 ± 3	105 ± 17 *	108 ± 6 *	39 ± 3	38 ± 3	94 ± 9	30 ± 4	26 ± 6	44 ± 4 *	<0.01	<0.01	0.02
Tyr	58 ± 4	83 ± 9	92 ± 9	35 ± 5	37 ± 4	64 ± 6	14 ± 3	21 ± 3	37 ± 2 *†	<0.01	<0.01	
Trp	17 ± 1	31 ± 3	27 ± 2	13 ± 1	15 ± 1	22 ± 3	8 ± 1	8 ± 1	11 ± 0 *†	<0.01	<0.01	<0.01

\* p < 0.05 vs cont.

† p < 0.05 vs 4 h.

mice, the glycogen metabolism pathway was also enriched. In contrast, pathways related to ketone body and cholesterol metabolism were enriched in UCP1-KO mice.

Pathway analysis showed the enhanced FA  $\beta$  oxidation both in WT and UCP1-KO mice (Fig. 4B). In addition, TG synthesis pathway were enhanced by cold exposure in both mice, suggesting the enhanced replenishment of intracellular lipid stores simultaneous with FA oxidation. Genes related to TG hydrolysis and FA uptake were upregulated both in WT and UCP1-KO mice (Fig. 4C). These data indicated that lipid metabolism was strongly enhanced by cold exposure in both mice. Interestingly, the expression of genes related to de novo FA synthesis were strongly induced in UCP1-KO mice, whereas Elov13 and 6, enzymes required for FA elongation that were reported to be important in BAT thermogenesis [36–38], were upregulated in both WT and UCP1-KO mice. The cold-induced enhancement of the expressions in *Acly*, *Acaca*, *Fasn*, and *Scd1* in UCP1-KO, but not in WT, mice were also confirmed by real-time PCR.

Genes related to alanine and aspartate metabolism were enriched by cold exposure in WT mice (Fig. 4B). Consistently, aspartate level tended to decrease upon cold exposure, but the effect was more robust in UCP1-KO mice (Fig. 3B). Gene expression of cytosolic aspartate aminotransferase (AST1), which catalyze the conversion of aspartate to oxaloacetic acid and is important for glyceroneogenesis [39], was highly induced in WT and UCP1-KO mice (Fig. 4D). In both mice, expressions of two enzyme involved in oxaloacetic acid metabolism, phosphoenolpyruvate carboxykinase 1 and malate dehydrogenase (MDH), were upregulated. In UCP1-KO mice, malic enzyme 1 (ME1) expression was significantly enhanced by cold exposure, suggesting that part of the aspartate-derived oxaloacetic acid was converted to pyruvic acid. Aspartate has been reported to be utilized for the production of *N*-acetyl-aspartate [40], but *N*-acetyl-aspartate synthetase (Asp-NAT, encoded by *Nat8l*), an enzyme responsible for this reaction, was actually decreased upon cold exposure in WT and UCP1-KO mice. However, aspartoacylase (ASPA) expression, which catalyzes the deacetylation of *N*-acetyl-aspartate and produces aspartate, was significantly induced only in WT mice.

Consistent with the increase in glutamine following cold exposure in WT, but not in UCP1-KO, mice (Fig. 3B), the expressions of genes encoding enzymes related to glutamine metabolism, such as glutaminase (GLS2) and glutamate dehydrogenase (GLUD1), were also increased by cold exposure in WT mice (Fig. 4E). Genes encoding glutamate

ammonia ligase (GLUL) was upregulated by cold exposure in both mice. Cold exposure showed significant or tendency of upregulation in the expression of gene encoding glutamate-cysteine ligase catalytic subunit (GCLC) and glutathione synthetase (GSS) in WT mice, suggesting that glutamine-derived glutamate was used for glutathione synthesis. Taken together, these results suggest active glutamine utilization in BAT of WT mice.

#### 4. Discussion

It is well known that BAT vigorously increases glucose utilization upon cold exposure. Glucose uptake is dependent on UCP1 thermogenesis [21], hence used in the detection of human brown fat by PET-CT [9,29–31]. On the other hand, some studies suggest that this method does not always reflect BAT activity. For example, human studies suggest that glucose uptake in BAT is partially dependent on insulin, because glucose accumulation in BAT is observed in lean, but not in insulin-resistant obese, subjects [30,31]. Indeed, insulin and cold stimulation enhance glucose uptake into human brown fat via distinct mechanisms [41]. In this study, we observed that glycolysis metabolites were increased after cold exposure in WT mice but were significantly decreased in UCP1-KO mice. In addition, lactic acid levels robustly increased by cold exposure in WT mice, suggesting that a large proportion of the glucose incorporated in BAT upon cold exposure is metabolized via anaerobic glycolysis. In UCP1-KO mice, cold exposure did not change lactic acid levels, although the basal level was rather high compared to WT mice. These results clearly showed that glycolysis and lactic acid production are enhanced as a result of UCP1-mediated thermogenesis. Notably, the levels of G-1-P, an initial substrate for glycogen synthesis, were significantly increased by cold exposure in WT, but not in UCP1-KO, mice. Consistent with this, gene enrichment analysis indicated the enhancement of glycogen metabolism in WT mice. Previous studies have demonstrated that BAT accumulates significant amounts of glycogen, although the effect of cold exposure on glycogen synthesis is controversial [42–44]. It is possible that the enhancement of glycogen synthesis occurs subsequent to enhanced glucose uptake, as glucose-derived G-6-P activates glycogen synthase via allosteric binding [45]. As previously reported [46], TCA cycle was accelerated after cold exposure in WT mice. In UCP1-KO mice, intermediates such as citric acid, aconic acid, and isocitric acid were increased upon

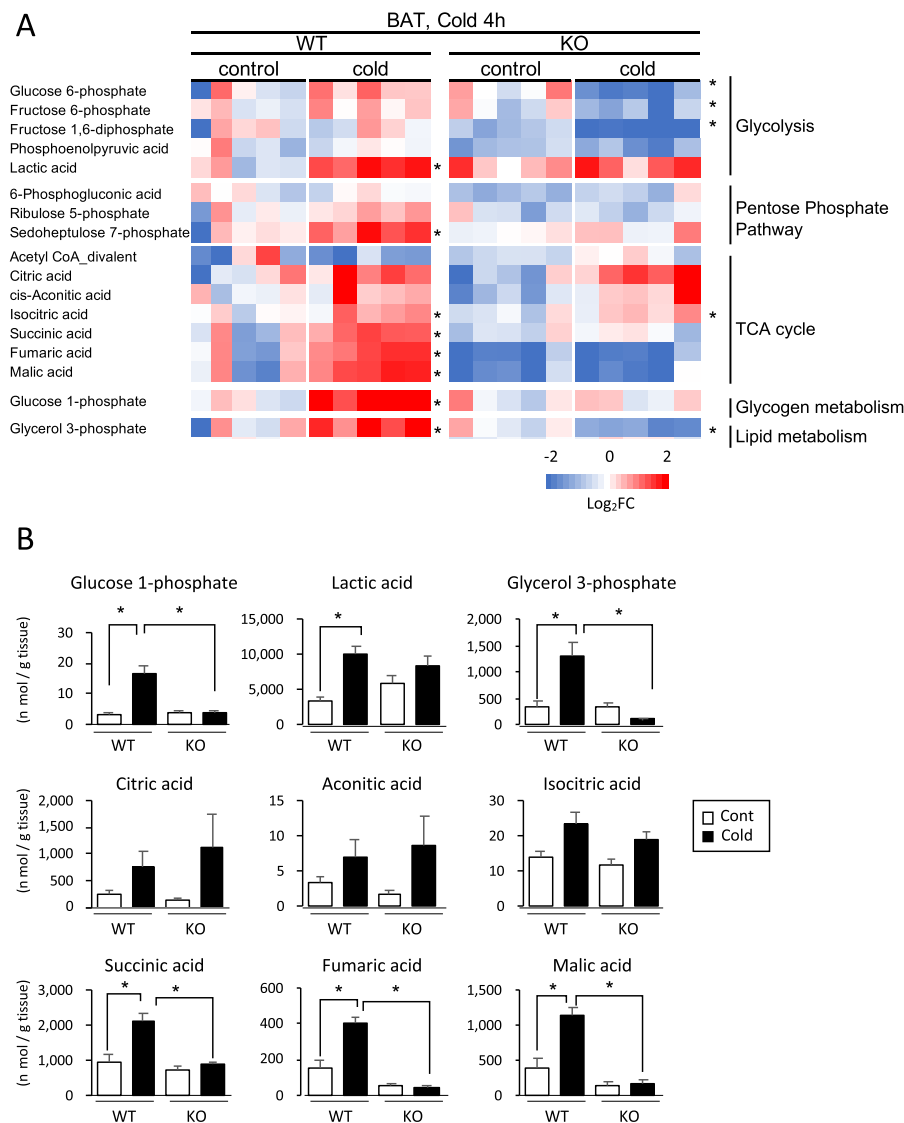


**Fig. 2.** Effect of cold exposure on carbohydrate metabolites in brown adipose tissue of wild-type and UCP1-KO mice. Male wild-type (WT) and UCP1-KO mice (10 weeks old) were exposed to cold (10 °C) for 4 h. Control mice were kept at room temperature (23 °C). Interscapular brown adipose tissue (BAT) was collected, and carbohydrate metabolites were analyzed. (A) The amount of each metabolites is expressed in a heat map as the log value of fold change compared to the value in BAT of control mice. \*  $p < 0.05$  compared to control group of each genotype (student's  $t$ -test). (B) Graphs for selected metabolites from panel (A). Values represent means  $\pm$  SE of 5 samples in each group. \* $p < 0.05$  (one-way ANOVA followed by Tukey's Honest Significant Difference test).

cold exposure, although intermediates downstream of  $\alpha$ -ketoglutaric acid were unchanged, suggesting that isocitrate dehydrogenase activity was inhibited by the high NADH/NAD ratio.

Pathway analysis of gene sets upregulated by cold exposure revealed active FA oxidation and TG synthesis in both genotypes of mice, indicating that cold-induced activation of these pathways is independent of UCP1-mediated thermogenesis. On the other hand, genes encoding key enzymes for de novo FA synthesis were greatly induced only in UCP1-KO mice. These results suggest that, in UCP1-KO mice, FA oxidation-derived acetyl-CoA was converted to citric acid and utilized for active de novo FA synthesis, in contrast to WT mice where FA oxidation-derived acetyl-CoA was oxidized through the TCA cycle and oxidative phosphorylation. It was reported that UCP1-KO mice can acclimate to cold environment by enhancing compensatory mechanisms of non-shivering thermogenesis independently of UCP1 [47]. In addition, a futile cycle of lipid oxidation and lipogenesis has been suggested as a mechanism of UCP1-independent thermogenesis in WAT [48]. Thus, it is plausible that the enhancement of both FA oxidation and synthesis in BAT of UCP1-KO mice may contribute to the UCP1-independent thermogenesis induced in compensation for the lack of

UCP1. In addition, this enhancement of de novo synthesis in UCP1-KO mice may explain the larger lipid accumulation in BAT compared to that in WT mice [10]. It is to be noted that de novo lipogenesis is reported in normal (WT) mice and rats when chronically exposed to cold environments [49–51]. Thus, acetyl-CoA is possibly consumed as a substrate for thermogenesis during an early phase of cold exposure and then for FA synthesis to replenish TG droplets during a later phase in WT mice.

Amino acid levels in BAT drastically changed upon cold exposure in both WT and UCP1-KO mice. In particular, we found that cold exposure significantly increased glutamine content specifically in WT mice but decreased aspartate and increased BCAAs specifically in UCP1-KO mice. It was unclear if these changes reflect uptake, utilization, production, or export of these amino acids. According to Lopez-Soriano et al. [25], higher glutamine content in WT mice is likely due to increased uptake. Indeed, adipose tissue is known to have active glutamine metabolism [52] and also contains high level of active GLS, an enzyme responsible for the conversion of glutamine to glutamate, reaching approximately 33% of the entire enzyme activity in rat lymphocytes or kidney [53]. Consistent with this, we observed that gene expression of GLS

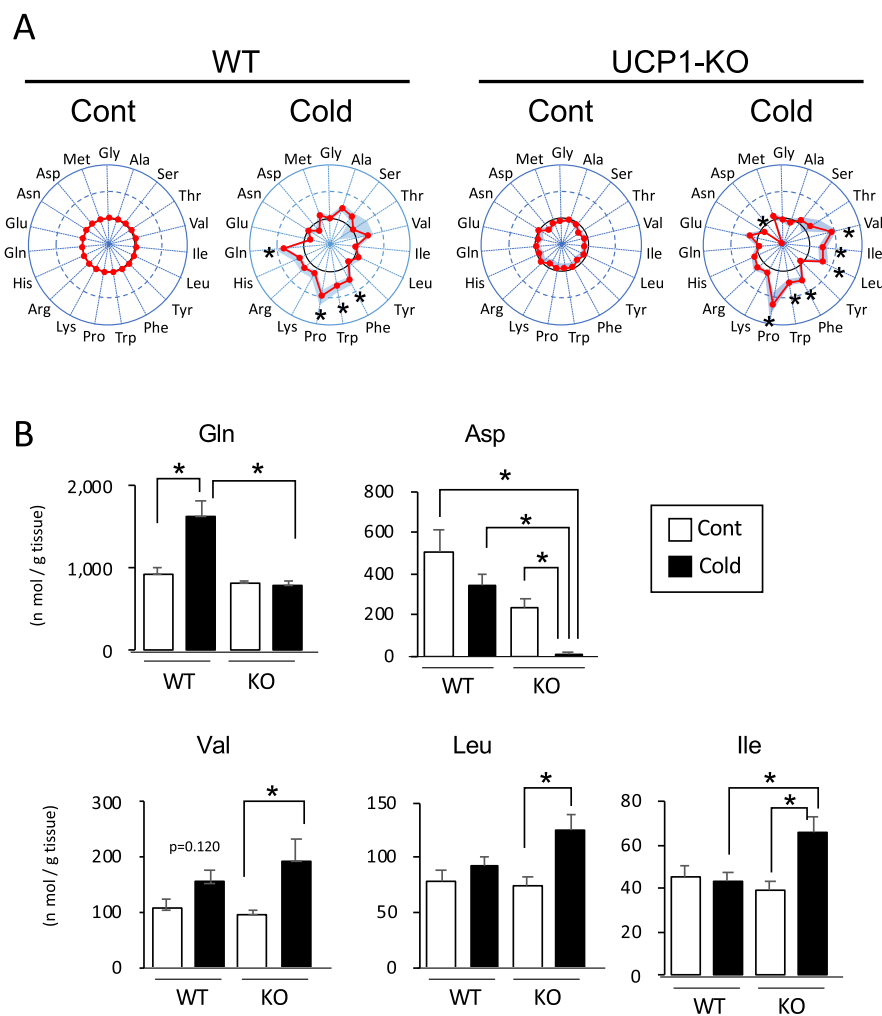


**Fig. 3.** Effect of cold exposure on amino acids in brown adipose tissue of wild-type and UCP1-KO mice. Male wild-type (WT) and UCP1-KO mice (10 weeks old) were exposed to cold (10 °C) for 4 h. Control mice were kept at room temperature (23 °C). Interscapular brown adipose tissue was collected, and amino acid content was analyzed. (A) Amino acids in tissue were expressed as fold change compared to the value in control WT mice. Small circles with a solid line and dotted lines indicate onefold and twofold expression, respectively. Values are expressed as means, and shaded areas indicate standard error,  $n = 5$ . \*  $p < 0.05$  compared to the control group of each genotype (student's *t*-test). (B) Graphs for select amino acids from panel (A). Values represent means  $\pm$  SE for 5 samples in each group. \* $p < 0.05$  (one-way ANOVA followed by Tukey's Honest Significant Difference test).

was increased after cold exposure in WT mice, supporting that the cold-induced increase of glutamine was due to the enhanced uptake from circulation. In cultured brown adipocytes, several lines of evidence have shown that glutamine was oxidized in response to  $\beta$ -AR stimulation [53,54], possibly through the conversion to  $\alpha$ -ketoglutaric acid, which enters TCA cycle. Consistent with this, the upregulation of the gene encoding GLUD1, an enzyme that catalyzes the production of  $\alpha$ -ketoglutaric acid from glutamate, was found in WT mice only. Collectively, these data suggest that glutamine is utilized as an important energy substrate for BAT thermogenesis *in vivo*. On the other hand, transcriptome analysis suggested that glutamine was also utilized for glutathione synthesis to defend against oxidative stress caused by high mitochondrial activity during thermogenesis. However, the contribution of this pathway to the total glutamine utilization seems to be relatively small; cold-induced increase in total glutathione (GSH and GSSG) was  $\sim 60$  nanomoles/g tissue, compared to the total increase in glutamine ( $\sim 700$  nanomoles/g tissue). Therefore, this pathway accounts for  $\sim 15\%$  of glutamine uptake in BAT upon cold exposure. It is unknown how UCP1-mediated thermogenesis induces glutamine uptake in BAT, but hypoxia induced by UCP1-mediated thermogenesis is plausibly involved in this regulation [55]. Hypoxia was reported to increase the uptake of glutamine, which is used for citrate production from  $\alpha$ -ketoglutaric acid [56] or *de novo* FA synthesis [57]. Although we did

not observe any change in the expression of glutamine transporter SLC1A5, a new mitochondrial isoform of SCL1A5 specifically induced by hypoxia was reported very recently [58]. Thus, further study is required to understand the mechanism and significance of cold-induced UCP1-dependent glutamine metabolism in BAT.

Pathway analysis of gene sets upregulated by cold exposure showed enhancement of alanine and aspartate metabolism in WT mice. Although these amino acid levels were not significantly changed, the expression of ASPA, an enzyme that produces aspartate from *N*-acetyl-aspartate, which is reported to be accumulated and affect lipid metabolism in BAT [40], was robustly upregulated by cold exposure in WT mice. In addition, we identified the cold-induced upregulation of AST1 expression, indicating the enhanced aspartate consumption. These results suggest that cold stimulation induces active aspartate turnover in BAT of WT mice. It was reported that aspartate is inefficiently transported into most mammalian cells [59], and that cold exposure has no effect on the uptake or release of aspartate after cold exposure in BAT of rats [25]. Therefore, it is possible that *N*-acetyl-aspartate serves as an aspartate source in BAT and compensates for the cold-induced loss of intracellular aspartate. In contrast to WT mice, ASPA expression was not affected in UCP1-KO mice, but AST1 was upregulated by cold exposure similar to WT mice. As AST1 was reported to play an important role in glyceroneogenesis

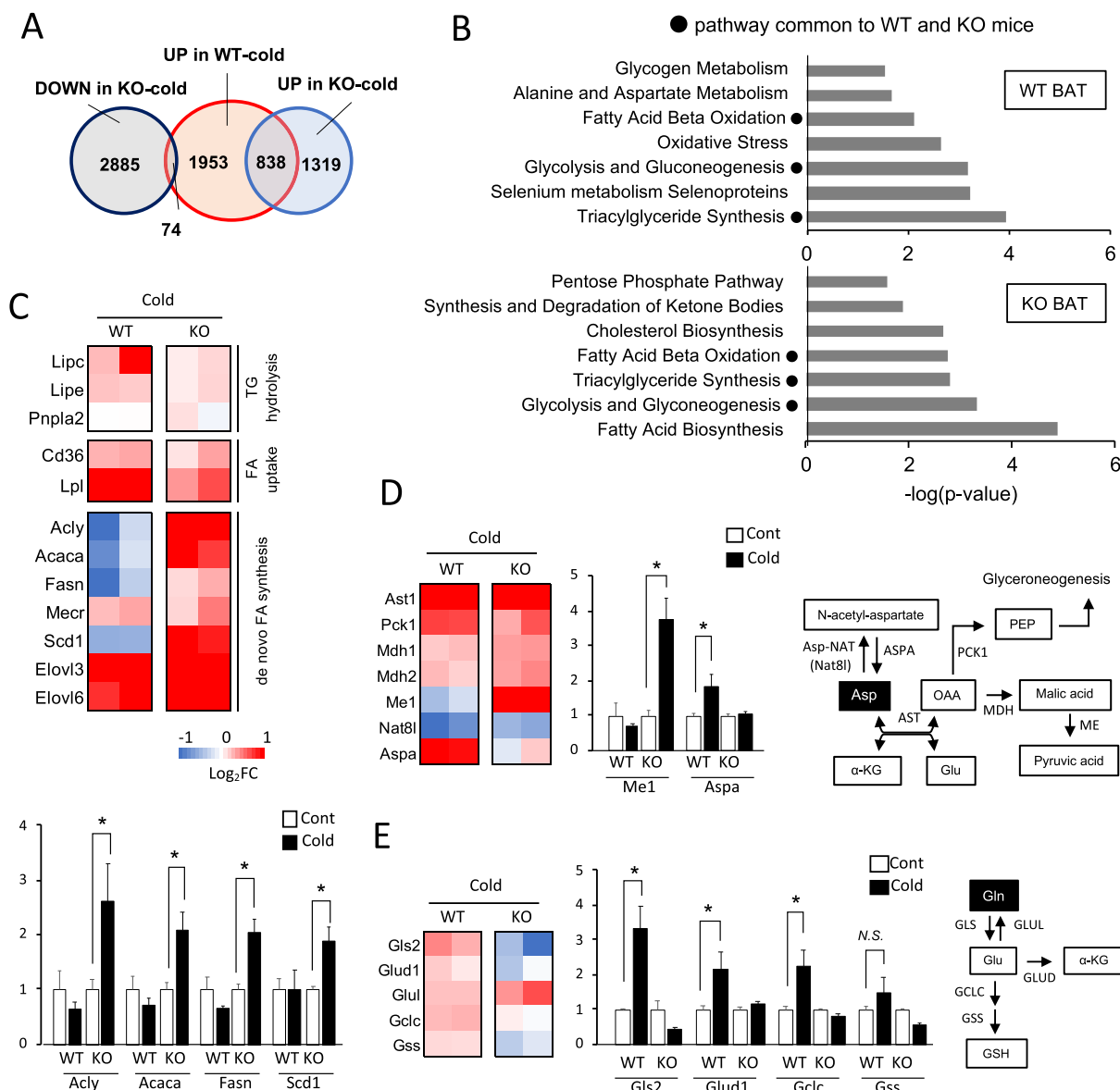


**Fig. 4.** Effect of cold exposure on gene expression in brown adipose tissue of wild-type and UCP1-KO mice. (A) Cold-induced changes in gene expression were analyzed by GeneChip array using brown adipose tissue samples in Figs. 2 and 3. (B) Pathway analysis of genes upregulated by cold exposure in wild-type (WT) mice or UCP1-KO mice. Heat maps were used to visualize the expression level of genes related to lipid (C), aspartate (D), and glutamine (E) metabolism as log values of fold changes compared to the values in control mice of each genotype. Real-time PCR was conducted to confirm the results of GeneChip array analysis. Expression levels were normalized to *TFIB* expression and expressed relative to the value of the control group of the same genotype. Values represent means  $\pm$  SE for 5 samples in each group. \* $p < 0.05$  (Student's *t*-test). (For interpretation of the references to color in this

in adipocytes [39,60], cold exposure may enhance the production of glycerol-3-phosphate from aspartate-derived oxaloacetic acid, simultaneous with the glycerol kinase pathway, irrespective of UCP1-mediated thermogenesis. Gene expression analysis suggested that oxaloacetic acid derived from aspartate was possibly metabolized by MDH to malic acid in mice of both genotypes. Malic acid possibly entered the actively accelerated TCA cycle in WT mice. In UCP1-KO mice, the upregulation of ME1 expression suggested that malic acid was converted to pyruvic acid, and NADPH produced through this cytosolic reaction may contribute to the active de novo FA synthesis. Thus, it is likely that aspartate utilization is enhanced by cold exposure irrespective of UCP1-mediated thermogenesis. The cold-induced drastic decrease in aspartate in BAT of UCP1-KO mice was possibly due to the lack of replenishment from *N*-acetyl-aspartate. Further study is required to understand the role of aspartate metabolism in BAT.

Gene enrichment analysis showed a weak but significant upregulation of the purine metabolism pathway (WT mice,  $p = 0.014$ ; UCP1-

KO mice,  $p = 0.032$ ) upon cold exposure. Therefore, it is also possible that aspartate was utilized as a precursor of purine nucleotides. It is well known that cold stimulation induces proliferation of preadipocytes and endothelial cells in BAT [3]. In addition, we previously reported that brown adipocytes also proliferate upon cold exposure [61] and that this proliferation is more rapidly induced after cold exposure than proliferation of stromal-vascular cells [62]. Upon active proliferation of these cells, synthesis of cellular components such as nucleotides, proteins and membrane phospholipids is required. Therefore, it is possible that a part of cold-induced metabolic changes in part support cell proliferation in BAT. Increased glutamine and enhanced pentose phosphate pathway-derived ribose-5-phosphate may also contribute to nucleotide synthesis, and high glycerol-3-phosphate may be used not only for TG synthesis but also for the phospholipid synthesis in WT mice.

We found that cold exposure significantly increased BCAAs specifically in UCP1-KO mice. Lopez-Soriano et al. reported that BCAAs are actively incorporated from the blood to BAT of cold-exposed rats [25]. A

recent study also revealed that BCAAs are actively utilized as a substrate for UCP1-mediated thermogenesis in mice [28]. Thus, it is plausible that BCAA incorporation in BAT is enhanced by cold exposure irrespective of UCP1-mediated thermogenesis but that their utilization is dependent on UCP1-mediated thermogenesis. Therefore, BCAAs incorporated in BAT were consumed for thermogenesis in WT mice but were accumulated in UCP1-KO mice due to the lack of thermogenesis.

In this study, we evaluated the cold-induced metabolic changes in relation to the UCP1-dependent thermogenesis. On the other hand, accumulating evidence has shown the mechanisms of UCP1-independent non-shivering thermogenesis in other tissues [47,63–67]. Thus, it cannot be ruled out that the metabolic changes observed in this study reflect such UCP1-independent thermogenesis in UCP1-KO mice. In addition, cellular metabolism may also be influenced by local temperature. Sympathetic activation of UCP1 increases BAT temperature by approximately 1.5 °C [10,21], whereas UCP1-KO mice become hypothermia and body temperature drops below 30 °C upon exposure to 4 °C [68]. Although we used milder cold condition (10 °C) in this study, the local temperature around BAT may substantially different between WT and UCP1-KO mice. Considering that temperature-dependent changes in glucose or fatty acid metabolism were reported in other tissues [69,70], it is possible that local temperature modifies cellular metabolism in BAT. Interestingly, thermo-sensitive transient receptor potential (TRP) channels were reported to be expressed in BAT [71], although it is unknown whether these channels in BAT actually respond to local temperature itself.

In summary, this study revealed that cold exposure induces metabolic pathways in WT and UCP1-KO mice, as illustrated in Fig. 5. In WT mice, cold exposure increases glycolysis, and pyruvic acid is metabolized via the TCA cycle and also lactic acid synthesis. Glutamine may provide  $\alpha$ -ketoglutaric acid to the TCA cycle, and also serve as a precursor of GSH to defend against oxidative stress caused by high mitochondrial activity. NADPH is produced through the active pentose phosphate pathway and is used for the reduction of GSSG. In UCP1-KO mice, glucose uptake does not increase upon cold exposure. Synthesis of FA and

TG is enhanced by cold exposure, contributing to the replenishment of intracellular TGs. Aspartate possibly contributes to the FA synthesis by supplying NADPH through its conversion first to oxaloacetic acid and then to pyruvate acid in the cytosol.

## 5. Conclusions

This study revealed that cold exposure induces UCP1-mediated thermogenesis-dependent glucose utilization and UCP1-independent active lipid metabolism. In addition, cold exposure largely affected amino acid metabolism in BAT, especially enhanced glutamine uptake dependent on UCP1-mediated thermogenesis. These results contribute to a comprehensive understanding of UCP1-mediated thermogenesis both dependent on and independent of BAT metabolism and revealed unique amino acid utilization in BAT. These results may provide useful information for the development of tracers for imaging of BAT activity.

## Funding

This study was supported by JSPS KAKENHI [grant Numbers 17K08118, 18H02274, and 19H04055].

## CRedit authorship contribution statement

**Yuko Okamatsu-Ogura:** Conceptualization, Investigation, Data curation, Writing - original draft, Visualization. **Masashi Kuroda:** Investigation, Data curation, Visualization. **Rie Tsutsumi:** Investigation, Data curation. **Ayumi Tsubota:** Investigation, Data curation. **Masayuki Saito:** Writing - review & editing. **Kazuhiro Kimura:** Writing - review & editing. **Hiroshi Sakaue:** Conceptualization, Writing - review & editing, Supervision.

## Declaration of competing interest

All authors declare no conflict of interest.

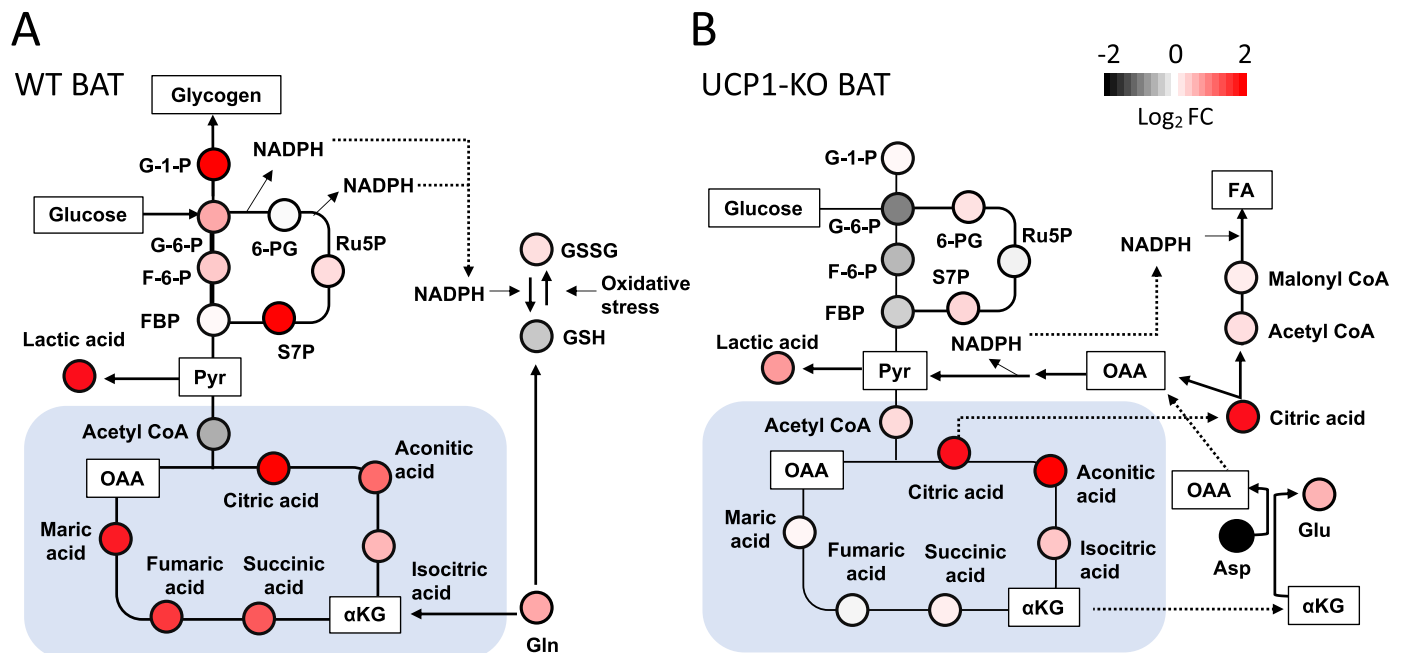


**Fig. 5.** Cold-induced metabolic pathways in wild-type and UCP1-KO mice. (A) In wild-type mice, cold exposure results in increased glycolysis, and pyruvic acid is metabolized through the TCA cycle and also synthesized into lactic acid. Glutamine provides  $\alpha$ -ketoglutaric acid to the TCA cycle and also serves as precursor of glutathione (GSH) to protect against oxidative stress caused by high mitochondrial activity. NADPH is produced via the active pentose phosphate pathway and used for the reduction of glutathione disulfide (GSSG). (B) In UCP1-KO mice, glucose uptake is not increased after cold exposure. Synthesis of FA and TG is enhanced by cold exposure, contributing to the replenishment of intracellular triglycerides. Aspartate may contribute to FA synthesis by supplying NADPH through the conversion to pyruvate in the cytosol.

## Acknowledgments

Y.O.O., K.M., R.T., and A.T. conducted the experiments; Y.O.O and H.S. designed the experiments; Y.O.O wrote the manuscript; M.S. and K.K gave conceptual advice on data interpretation. This work was supported by The Special Mission Center for Metabolome Analysis, school of medical nutrition, Faculty of Medicine of Tokushima University.

## References

- Cinti S. The role of brown adipose tissue in human obesity. *Nutr Metab Cardiovasc Dis.* 2006;16(8):569–74. <https://doi.org/10.1016/j.numecd.2006.07.009>.
- Harms M, Seale P. Brown and beige fat: development, function and therapeutic potential. *Nat Med.* 2013;19(10):1252–63. <https://doi.org/10.1038/nm.3361>.
- Cannon B, Nedergaard J. Brown adipose tissue: function and physiological significance. *Physiol Rev.* 2004;84(1):277–359. <https://doi.org/10.1152/physrev.00015.2003>.
- Lkhagvasuren B, Nakamura Y, Oka T, Sudo N, Nakamura K. Social defeat stress induces hyperthermia through activation of thermoregulatory sympathetic premotor neurons in the medullary raphe region. *Eur J Neurosci.* 2011;34(9):1442–52. <https://doi.org/10.1111/j.1460-9568.2011.07863.x>.
- Kataoka N, Hioki H, Kaneko T, Nakamura K. Psychological stress activates a dorsomedial hypothalamus-medullary raphe circuit driving brown adipose tissue thermogenesis and hyperthermia. *Cell Metab.* 2014;20(2):346–58. <https://doi.org/10.1016/j.cmet.2014.05.018>.
- Enerback S, Jacobsson A, Simpson EM, Guerra C, Yamashita H, Harper ME, et al. Mice lacking mitochondrial uncoupling protein are cold-sensitive but not obese. *Nature.* 1997;387(6628):90–4. <https://doi.org/10.1038/387090a0>.
- Tsubota A, Okamatsu-Ogura Y, Bariuan JV, Mae J, Matsuoka S, Nio-Kobayashi J, et al. Role of brown adipose tissue in body temperature control during the early postnatal period in Syrian hamsters and mice. *J Vet Med Sci.* 2019;81(10):1461–7. <https://doi.org/10.1292/jvms.19-0371>.
- Saito M, Matsushita M, Yoneshiro T, Okamatsu-Ogura Y. Brown adipose tissue, diet-induced thermogenesis, and thermogenic food ingredients: from mice to men. *Front Endocrinol (Lausanne).* 2020;11:222. <https://doi.org/10.3389/fendo.2020.00222>.
- Saito M, Okamatsu-Ogura Y, Matsushita M, Watanabe K, Yoneshiro T, Nio-Kobayashi J, et al. High incidence of metabolically active brown adipose tissue in healthy adult humans: effects of cold exposure and adiposity. *Diabetes.* 2009;58(7):1526–31. <https://doi.org/10.2337/db09-0530>.
- Inokuma K, Okamatsu-Ogura Y, Omachi A, Matsushita Y, Kimura K, Yamashita H, et al. Indispensable role of mitochondrial UCP1 for antiobesity effect of beta3-adrenergic stimulation. *Am J Physiol Endocrinol Metab.* 2006;290(5):E1014–21. <https://doi.org/10.1152/ajpendo.00105.2005>.
- Feldmann HM, Golozoubova V, Cannon B, Nedergaard J. UCP1 ablation induces obesity and abolishes diet-induced thermogenesis in mice exempt from thermal stress by living at thermoneutrality. *Cell Metab.* 2009;9(2):203–9. <https://doi.org/10.1016/j.cmet.2008.12.014>.
- Fedorenko A, Lishko PV, Kirichok Y. Mechanism of fatty-acid-dependent UCP1 uncoupling in brown fat mitochondria. *Cell.* 2012;151(2):400–13. <https://doi.org/10.1016/j.cell.2012.09.010>.
- Divakaruni AS, Humphrey DM, Brand MD. Fatty acids change the conformation of uncoupling protein 1 (UCP1). *J Biol Chem.* 2012;287(44):36845–53. <https://doi.org/10.1074/jbc.M112.381780>.
- Bartelt A, Bruns OT, Reimer R, Hohenberg H, Itrich H, Peldschus K, et al. Brown adipose tissue activity controls triglyceride clearance. *Nat Med.* 2011;17(2):200–5. <https://doi.org/10.1038/nm.2297>.
- Khedoe PP, Hoeke G, Kooijman S, Dijk W, Buijs JT, Kersten S, et al. Brown adipose tissue takes up plasma triglycerides mostly after lipolysis. *J Lipid Res.* 2015;56(1):51–9. <https://doi.org/10.1194/jlr.M052746>.
- Labbe SM, Caron A, Bakan I, Laplante M, Carpentier AC, Lecomte R, et al. In vivo measurement of energy substrate contribution to cold-induced brown adipose tissue thermogenesis. *FASEB J.* 2015;29(5):2046–58. <https://doi.org/10.1096/fj.14-266247>.
- Blondin DP, Frisch F, Phoenix S, Guerin B, Turcotte EE, Haman F, et al. Inhibition of intracellular triglyceride lipolysis suppresses cold-induced brown adipose tissue metabolism and increases shivering in humans. *Cell Metab.* 2017;25(2):438–47. <https://doi.org/10.1016/j.cmet.2016.12.005>.
- Schreiber R, Diwoky C, Schoiswohl G, Feiler U, Wongsiriroj N, Abdellatif M, et al. Cold-induced thermogenesis depends on ATGL-mediated lipolysis in cardiac muscle, but not brown adipose tissue. *Cell Metab.* 2017;26(5):753–63. <https://doi.org/10.1016/j.cmet.2017.09.004>.
- Shin H, Ma Y, Chanturiya T, Cao Q, Wang Y, Kagedowda AKG, et al. Lipolysis in brown adipocytes is not essential for cold-induced thermogenesis in mice. *Cell Metab.* 2017;26(5):764–77. <https://doi.org/10.1016/j.cmet.2017.09.002>.
- Shimizu Y, Nikami H, Saito M. Sympathetic activation of glucose utilization in brown adipose tissue in rats. *J Biochem.* 1991;110(5):688–92. <https://doi.org/10.1093/oxfordjournals.jbchem.a123642>.
- Inokuma K, Ogura-Okamatsu Y, Toda C, Kimura K, Yamashita H, Saito M. Uncoupling protein 1 is necessary for norepinephrine-induced glucose utilization in brown adipose tissue. *Diabetes.* 2005;54(5):1385–91. <https://doi.org/10.2337/diabetes.54.5.1385>.
- Teperino R, Amann S, Bayer M, McGee SL, Loipetzberger A, Connor T, et al. Hedgehog partial agonism drives Warburg-like metabolism in muscle and brown fat. *Cell.* 2012;151(2):414–26. <https://doi.org/10.1016/j.cell.2012.09.021>.
- Winther S, Isidor MS, Basse AL, Skjoldborg N, Cheung A, Quistorff B, et al. Restricting glycolysis impairs brown adipocyte glucose and oxygen consumption. *Am J Physiol Endocrinol Metab.* 2018;314(3):E214–E23. <https://doi.org/10.1152/ajpendo.00218.2017>.
- Jeong JH, Chang JS, Jo YH. Intracellular glycolysis in brown adipose tissue is essential for optogenetically induced nonshivering thermogenesis in mice. *Sci Rep.* 2018;8(1):6672. <https://doi.org/10.1038/s41598-018-25265-3>.
- Lopez-Soriano FJ, Fernandez-Lopez JA, Mampel T, Villarroya F, Iglesias R, Alemany M. Amino acid and glucose uptake by rat brown adipose tissue. Effect of cold-exposure and acclimation. *Biochem J.* 1988;252(3):843–9. <https://doi.org/10.1042/bj2520843>.
- Lopez-Soriano FJ, Alemany M. Effect of cold-temperature exposure and acclimation on amino acid pool changes and enzyme activities of rat brown adipose tissue. *Biochim Biophys Acta.* 1987;925(3):265–71. [https://doi.org/10.1016/0304-4165\(87\)90191-7](https://doi.org/10.1016/0304-4165(87)90191-7).
- Lu X, Solmonson A, Lodi A, Nowinski SM, Sentandreu E, Riley CL, et al. The early metabolomic response of adipose tissue during acute cold exposure in mice. *Sci Rep.* 2017;7(1):3455. <https://doi.org/10.1038/s41598-017-03108-x>.
- Yoneshiro T, Wang Q, Tajima K, Matsushita M, Maki H, Igarashi K, et al. BCAA catabolism in brown fat controls energy homeostasis through SLC25A44. *Nature.* 2019;572(7771):614–9. <https://doi.org/10.1038/s41586-019-1503-x>.
- Virtanen KA, Lidell ME, Orava J, Heglind M, Westergren R, Niemi T, et al. Functional brown adipose tissue in healthy adults. *N Engl J Med.* 2009;360(15):1518–25. <https://doi.org/10.1056/NEJMoa0808949>.
- van Marken Lichtenbelt WD, Vanhomerig JW, Smulders NM, Drossaerts JM, Kemerink GJ, Bouvy ND, et al. Cold-activated brown adipose tissue in healthy men. *N Engl J Med.* 2009;360(15):1500–8. <https://doi.org/10.1056/NEJMoa0808718>.
- Cypess AM, Lehman S, Williams G, Tal I, Rodman D, Goldfine AB, et al. Identification and importance of brown adipose tissue in adult humans. *N Engl J Med.* 2009;360(15):1509–17. <https://doi.org/10.1056/NEJMoa0810780>.
- Heine M, Fischer AW, Schlein C, Jung C, Straub LG, Gottschling K, et al. Lipolysis triggers a systemic insulin response essential for efficient energy replenishment of activated brown adipose tissue in mice. *Cell Metab.* 2018;28(4):644–55. <https://doi.org/10.1016/j.cmet.2018.06.020>.
- UD M, Saari T, Raiko J, Kudomi N, Maurer SF, Laheesmaa M, et al. Postprandial oxidative metabolism of human brown fat indicates thermogenesis. *Cell Metab.* 2018;28(2):207–16. <https://doi.org/10.1016/j.cmet.2018.05.020>.
- Miyake M, Kuroda M, Kiyonari H, Takehana K, Hisanaga S, Morimoto M, et al. Ligand-induced rapid skeletal muscle atrophy in HSA-Fv2E-PERK transgenic mice. *PLoS One.* 2017;12(6):e0179955. <https://doi.org/10.1371/journal.pone.0179955>.
- Soga T, Heiger DN. Amino acid analysis by capillary electrophoresis electrospray ionization mass spectrometry. *Anal Chem.* 2000;72(6):1236–41. <https://doi.org/10.1021/ac990976y>.
- Tvrđik P, Asadi A, Kozak LP, Nedergaard J, Cannon B, Jacobsson A. Cig30, a mouse member of a novel membrane protein gene family, is involved in the recruitment of brown adipose tissue. *J Biol Chem.* 1997;272(50):31738–46. <https://doi.org/10.1074/jbc.272.50.31738>.
- Westerberg R, Mansson JE, Golozoubova V, Shabalina IG, Backlund EC, Tvrđik P, et al. ELOVL3 is an important component for early onset of lipid recruitment in brown adipose tissue. *J Biol Chem.* 2006;281(8):4958–68. <https://doi.org/10.1074/jbc.M511588200>.
- Tan CY, Virtue S, Bidault G, Dale M, Hagen R, Griffin JL, et al. Brown adipose tissue thermogenic capacity is regulated by Elovl6. *Cell Rep.* 2015;13(10):2039–47. <https://doi.org/10.1016/j.celrep.2015.11.004>.
- Tordjiman J, Leroyer S, Chauvet G, Quette J, Chauvet C, Tomkiewicz C, et al. Cytosolic aspartate aminotransferase, a new partner in adipocyte glyceroneogenesis and an atypical target of thiazolidinedione. *J Biol Chem.* 2007;282(32):23591–602. <https://doi.org/10.1074/jbc.M611111200>.
- Huber K, Hofer DC, Trefely S, Pelzmann HJ, Madreiter-Sokolowski C, Duta-Mare M, et al. N-acetylaspartate pathway is nutrient responsive and coordinates lipid and energy metabolism in brown adipocytes. *Biochim Biophys Acta Mol Cell Res.* 2019;1866(3):337–48. <https://doi.org/10.1016/j.bbamcr.2018.08.017>.
- Orava J, Nuutila P, Lidell ME, Oikonen V, Noponen T, Viljanen T, et al. Different metabolic responses of human brown adipose tissue to activation by cold and insulin. *Cell Metab.* 2011;14(2):272–9. <https://doi.org/10.1016/j.cmet.2011.06.012>.
- Carmean CM, Bobe AM, Yu JC, Volden PA, Brady MJ. Refeeding-induced brown adipose tissue glycogen hyper-accumulation in mice is mediated by insulin and catecholamines. *PLoS One.* 2013;8(7):e67807. <https://doi.org/10.1371/journal.pone.0067807>.
- Madar Z, Harel A. Does the glycogen synthase (EC 2.4.1.21) of brown adipose tissue play a regulatory role in glucose homeostasis? *Br J Nutr.* 1991;66(1):95–104. <https://doi.org/10.1079/bjn19910013>.
- Farkas V, Kelenyi G, Sandor A. A dramatic accumulation of glycogen in the brown adipose tissue of rats following recovery from cold exposure. *Arch Biochem Biophys.* 1999;365(1):54–61. <https://doi.org/10.1006/abbi.1999.1157>.
- Villar-Palasi C, Guinovart JJ. The role of glucose 6-phosphate in the control of glycogen synthase. *FASEB J.* 1997;11(7):544–58.
- Hao Q, Yadav R, Basse AL, Petersen S, Sonne SB, Rasmussen S, et al. Transcriptome profiling of brown adipose tissue during cold exposure reveals extensive regulation of glucose metabolism. *Am J Physiol Endocrinol Metab.* 2015;308(5):E380–92. <https://doi.org/10.1152/ajpendo.00277.2014>.
- Ukropec J, Anunciado RP, Ravussin Y, Hulver MW, Kozak LP. UCP1-independent thermogenesis in white adipose tissue of cold-acclimated Ucp1<sup>-/-</sup> mice. *J Biol Chem.* 2006;281(42):31894–908. <https://doi.org/10.1074/jbc.M606114200>.
- Granneman JG, Burnazi M, Zhu Z, Schwamb LA. White adipose tissue contributes to UCP1-independent thermogenesis. *Am J Physiol Endocrinol Metab.* 2003;285(6):E1230–6. <https://doi.org/10.1152/ajpendo.00197.2003>.

- [49] Yu XX, Lewin DA, Forrest W, Adams SH. Cold elicits the simultaneous induction of fatty acid synthesis and beta-oxidation in murine brown adipose tissue: prediction from differential gene expression and confirmation in vivo. *FASEB J*. 2002;16(2):155–68. <https://doi.org/10.1096/fj.01-0568com>.
- [50] Moura MA, Festuccia WT, Kawashita NH, Garofalo MA, Brito SR, Kettelhut IC, et al. Brown adipose tissue glyceroneogenesis is activated in rats exposed to cold. *Pflügers Arch*. 2005;449(5):463–9. <https://doi.org/10.1007/s00424-004-1353-7>.
- [51] Mottillo EP, Balasubramanian P, Lee YH, Weng C, Kershaw EE, Granneman JG. Coupling of lipolysis and de novo lipogenesis in brown, beige, and white adipose tissues during chronic beta3-adrenergic receptor activation. *J Lipid Res*. 2014;55(11):2276–86. <https://doi.org/10.1194/jlr.M050005>.
- [52] Ritchie JW, Baird FE, Christie GR, Stewart A, Low SY, Hundal HS, et al. Mechanisms of glutamine transport in rat adipocytes and acute regulation by cell swelling. *Cell Physiol Biochem*. 2001;11(5):259–70. <https://doi.org/10.1159/000047812>.
- [53] Kowalchuk JM, Curi R, Newsholme EA. Glutamine metabolism in isolated incubated adipocytes of the rat. *Biochem J*. 1988;249(3):705–8. <https://doi.org/10.1042/bj2490705>.
- [54] Held NM, Kuipers EN, van Weeghel M, van Klinken JB, Denis SW, Lombes M, et al. Pyruvate dehydrogenase complex plays a central role in brown adipocyte energy expenditure and fuel utilization during short-term beta-adrenergic activation. *Sci Rep*. 2018;8(1):9562. <https://doi.org/10.1038/s41598-018-27875-3>.
- [55] Xue Y, Petrovic N, Cao R, Larsson O, Lim S, Chen S, et al. Hypoxia-independent angiogenesis in adipose tissues during cold acclimation. *Cell Metab*. 2009;9(1):99–109. <https://doi.org/10.1016/j.cmet.2008.11.009>.
- [56] Wise DR, Ward PS, Shay JE, Cross JR, Gruber JJ, Sachdeva UM, et al. Hypoxia promotes isocitrate dehydrogenase-dependent carboxylation of alpha-ketoglutarate to citrate to support cell growth and viability. *Proc Natl Acad Sci U S A*. 2011;108(49):19611–6. <https://doi.org/10.1073/pnas.1117773108>.
- [57] Metallo CM, Gameiro PA, Bell EL, Mattaini KR, Yang J, Hiller K, et al. Reductive glutamine metabolism by IDH1 mediates lipogenesis under hypoxia. *Nature*. 2011;481(7381):380–4. <https://doi.org/10.1038/nature10602>.
- [58] Yoo HC, Park SJ, Nam M, Kang J, Kim K, Yeo JH, et al. A variant of SLC1A5 is a mitochondrial glutamine transporter for metabolic reprogramming in cancer cells. *Cell Metab*. 2020;31(2):267–83 e12. <https://doi.org/10.1016/j.cmet.2019.11.020>.
- [59] Birsoy K, Wang T, Chen WW, Freinkman E, Abu-Remaileh M, Sabatini DM. An essential role of the mitochondrial electron transport chain in cell proliferation is to enable aspartate synthesis. *Cell*. 2015;162(3):540–51. <https://doi.org/10.1016/j.cell.2015.07.016>.
- [60] Franckhauser S, Munoz S, Pujol A, Casellas A, Riu E, Otaegui P, et al. Increased fatty acid re-esterification by PEPCK overexpression in adipose tissue leads to obesity without insulin resistance. *Diabetes*. 2002;51(3):624–30. <https://doi.org/10.2337/diabetes.51.3.624>.
- [61] Okamatsu-Ogura Y, Fukano K, Tsubota A, Nio-Kobayashi J, Nakamura K, Morimatsu M, et al. Cell-cycle arrest in mature adipocytes impairs BAT development but not WAT browning, and reduces adaptive thermogenesis in mice. *Sci Rep*. 2017;7(1):6648. <https://doi.org/10.1038/s41598-017-07206-8>.
- [62] Fukano K, Okamatsu-Ogura Y, Tsubota A, Nio-Kobayashi J, Kimura K. Cold exposure induces proliferation of mature brown adipocyte in a ss3-adrenergic receptor-mediated pathway. *PLoS One*. 2016;11(11):e0166579. <https://doi.org/10.1371/journal.pone.0166579>.
- [63] Bal NC, Maurya SK, Sopariwala DH, Sahoo SK, Gupta SC, Shaikh SA, et al. Sarcolipin is a newly identified regulator of muscle-based thermogenesis in mammals. *Nat Med*. 2012;18(10):1575–9. <https://doi.org/10.1038/nm.2897>.
- [64] Ikeda K, Kang Q, Yoneshiro T, Camporez JP, Maki H, Homma M, et al. UCP1-independent signaling involving SERCA2b-mediated calcium cycling regulates beige fat thermogenesis and systemic glucose homeostasis. *Nat Med*. 2017;23(12):1454–65. <https://doi.org/10.1038/nm.4429>.
- [65] Ukropec J, Anunciado RV, Ravussin Y, Kozak LP. Leptin is required for uncoupling protein-1-independent thermogenesis during cold stress. *Endocrinology*. 2006;147(5):2468–80. <https://doi.org/10.1210/en.2005-1216>.
- [66] Bertholet AM, Chouchani ET, Kazak L, Angelin A, Fedorenko A, Long JZ, et al. H(+) transport is an integral function of the mitochondrial ADP/ATP carrier. *Nature*. 2019;571(7766):515–20. <https://doi.org/10.1038/s41586-019-1400-3>.
- [67] Kazak L, Chouchani ET, Jedrychowski MP, Erickson BK, Shinoda K, Cohen P, et al. A creatine-driven substrate cycle enhances energy expenditure and thermogenesis in beige fat. *Cell*. 2015;163(3):643–55. <https://doi.org/10.1016/j.cell.2015.09.035>.
- [68] Golozoubova V, Hohtola E, Matthias A, Jacobsson A, Cannon B, Nedergaard J. Only UCP1 can mediate adaptive nonshivering thermogenesis in the cold. *FASEB J*. 2001;15(11):2048–50. <https://doi.org/10.1096/fj.00-0536fje>.
- [69] Zoladz JA, Koziel A, Broniarek I, Woyda-Ploszczycza AM, Ogrodna K, Majerczak J, et al. Effect of temperature on fatty acid metabolism in skeletal muscle mitochondria of untrained and endurance-trained rats. *PLoS One*. 2017;12(12):e0189456. <https://doi.org/10.1371/journal.pone.0189456>.
- [70] Hall PF, Nakamura M. Influence of temperature on hexose transport by round spermatids of rats. *J Reprod Fertil*. 1981;63(2):373–9. <https://doi.org/10.1530/jrf.0.0630373>.
- [71] Uchida K, Dezaki K, Yoneshiro T, Watanabe T, Yamazaki J, Saito M, et al. Involvement of thermosensitive TRP channels in energy metabolism. *J Physiol Sci*. 2017;67(5):549–60. <https://doi.org/10.1007/s12576-017-0552-x>.